Enhancement of optical bandwidth in altermagnets

M.Sc. Thesis

by

Shubhranshu Dwivedi

DEPARTMENT OF PHYSICS

INDIAN INSTITUTE OF TECHNOLOGY INDORE

MAY 2024

Enhancement of optical bandwidth in altermagnets

A THESIS

Submitted in partial fulfillment of the requirements for the award of the degree of

Master of Science

by

Shubhranshu Dwivedi

(Roll No.2203151020)

Under the guidance of

Dr.Alestin Mawrie

DEPARTMENT OF PHYSICS

INDIAN INSTITUTE OF TECHNOLOGY INDORE

MAY 2024

INDIAN INSTITUTE OF TECHNOLOGY INDORE

CANDIDATE'S DECLARATION

I hereby certify that the work which is being presented in the thesis entitled **"Enhancement of optical bandwidth in altermagnets"** in the partial fulfillment of the requirements for the award of the degree of **MASTER OF SCIENCE** and submitted in the **DEPARTMENT OF PHYSICS**, **Indian Institute of Technology Indore**, is an authentic record of my own work carried out during the time period from July 2023 to May 2024 under the supervision of **Dr.Alestin Mawrie**, Assistant Professor, Department of Physics, IIT Indore. The matter presented in this thesis by me has not been submitted for the award of any other degree of this or any other institute.

Shubhranshu

Signature of the student with date

(**Shubhranshu Dwivedi**)

This is to certify that the above statement made by the candidate is correct to the best of my knowledge.

Mawrie
15/05/2024

Signature of Thesis Supervisor with date

(**Dr.Alestin Mawrie**)

Shubhranshu Dwivedi has successfully given his M.Sc. Oral Examination held on 15$^{\text{th}}$ May, 2024.

Signature of supervisor of M.Sc Thesis

Date:

Signature of DPGC

Date:

,

Dedicated to
my beloved parents and family.

"What you need, above all else, is a love for your subject, whatever it is. You've got to be so deeply in love with your subject that when curve balls are thrown, when hurdles are put in place, you've got the ; l' energy to overcome them." –***Neil deGrasse Tyson***

Acknowledgements

I am incredibly grateful to my supervisor, Dr. Alestin Mawrie, for his assistance and guidance throughout my M.Sc. period. With his kind support and guidance, my M.Sc. journey has been enthusiastic and has motivated me for the future. His method of observing problems and breaking them down motivates me to look at issues differently. I am completing my M.Sc. with much more maturity in mathematics and physics compared to when I began, and his role in this journey has been magnificent. I extend my thanks to DPGC convener Dr. Dipankar Das, HOD Dr. Preeti Bhobhe and all of my teachers for their kind and valuable suggestions. I am also thankful to Ph.D. scholar Sushmita Saha for clearing my doubts related to my thesis and academics. Despite having busy schedules, she always made time for discussion and helped me whenever I needed it.

I would like to thank my family for being my backbone throughout my academic journey. Their support is always there for me, making me feel blessed and motivated. It is their trust in me and their love that has helped me overcome all the academic and emotional challenges I have faced during my master's.

Abstract

The realization of the unconventional d-wave magnetism in materials necessitates a $\mathbf{k} \cdot \mathbf{p}$ Rashba Hamiltonian added to the altermagnetic two-band Hamiltonian. This brings about a two spin-split bands system with spin-orbit coupling (SOC) gap minimum about the azimurthal direction $\phi_{\mathbf{k}} = n\pi/2$ (where the spin-vectors are tangential to the (k_x, k_y) plane) and it is found to be maximum about the direction $\phi_{\mathbf{k}} = (2n+1)\pi/4$ (where the z-component of the spin vectors is maximum). We show in this thesis that the alternating spin-momentum coupling in altermagnets initiates an enhancement in the optical bandwidth of the system, a phenomena similar to that provided by the Dresselhaus SOC in semiconductor with bulk inversion asymmetry. In manifestation with the observation listed above, the optical conductivity displays a van-Hove singularity at points about the directions $\phi_{\mathbf{k}} = n\pi/2$ and $\phi_{\mathbf{k}} = (2n+1)\pi/4$ showing extrema whenever the frequecy is such that $\Omega = 2(E_+ - E_-)_{k_F(\phi_{\mathbf{k}})}$.

List of Figures

Contents

Introduction

There is a recent theoretical and experimental development of a new class of magnetic materials called altermagnets with net-zero magnetization similar to antiferromagnets upon application of an electric field. The distinctive feature of generation of a net spin current on the application of a voltage bias in a junction of metal and an altermagnet, is what sets them apart from the antiferromagnetic materials. In some altermagnets there has been a realization of unconventional d-wave magnetism, a long-sought after magnetic counterpart of d-wave superconductivity that has opened up new research directions in countering the interplay between the magnetism and superconductivity, moreover, few fundamental spintronics effects like Giant and tunneling magnetoresistence which are physical phenomena used for reading information in spintronics devices makes this new phase of material a good candidate of ongoing research in condensed matter physics. The altermagnetism phenomenon has been shown to occur in abundant in both three-dimensional and two-dimensional crystals in recent studies.

This new phase of magnetic material is characterized by its anisotropic spin-polarized bands, which leads to a predicted altermagnetic electron quasiparticle that can be illustrated on a two-band model Hamiltonian that we are going to present in Chapter 1. In order to predict unique elements of the Berry phase phenomenon in such altermagnets we model the Γ-point by a $k \cdot p$ Rashba model. The Rashba term is gate-voltage dependent and generates spin-up/down imbalance in the system thus directly anticipating the non-zero magnetization in antiferromagnets upon application of an electric field. Thus, the Rashba effect provides us with a necessary means to accumulate spin population imbalance in the system, boasting the scope of these materials in terms of spin transfer torque (STT) application.

Apart from that, it has been realized that time-reversal symmetry breaking in altermagnetic materials gives rise to the spontaneous Hall effect and thus non-zero Hall conductivity. In this work, we present a study of the optical conductivity in the altermagnetic materials taking into account the Rashba-spin orbit coupling phenomena. The spin-exchange parameter increases the optical spectrum of altermagnets. Our work in this regard is organized by introducing physical phenomenon like time-reversal symmetry breaking and large Berry curvature in altermagnets with the theoretical study of the electron-quasi particle Hamiltonian in a tight-binding approach (chapter 1). In chapter 2 we present a formulation of the Optical conductivity tensor with the application of the Matsubara frequency summation technique and derive the Rashba spin-orbit term needed to assign the ground state Hamiltonian. The concluding remark of our work followed by the detailed calculation of AC and DC conductivity and joint density of states is presented in Chapter 3.

CHAPTER 1

Altermagnetism: New phase of magnetic materials

1.1 Beyond conventional magnetism

Traditionally we know about the two types of magnetic phases i.e ferromagnets and antiferromagnets. Ferromagnets are charecterized by electronic band structures with spin splitting and broken time seversal symmetry, while on the other hand in antiferromagnets, a compensating antiparallel ordering of atomic magnetic moments in direct physical space leads to the absence of net magnetisation. The altermagnetism is a new type of magnetism in which the directions of the atomic magnetic moments alter in periodic configurations creating the local polarization of the field. It has been theroretically predicted that few crystals with compensated antiparallel magnetic ordering which is characterstic of antiferromagnets, preserve the inversion symmetry while breaking time reversal symmetry with the spin splitted band structure which is similar to the ferromagnets. This apparent ferromagnetic-antiferromagnetic dichotomy in these materials is

identified as a new magnetic phase which we call **Altermagnetism**.
This new phase can be seen in 2D and 3D crystals while the realization of altermagnetism in 1D is prohibited because rotation transformations are absent in 1D. Researchers have experimentally identified altermagnetic candidates that cover the large range of materials from metals, semimetals to semiconductors and superconductors. An illustration of three non-relativistic magnetic phases is shown in Fig.[1.1] with their band structure and energy isosurfaces. The spin-split band structures of altermagnetic materials are depicted in Fig.[1.1(d)] .

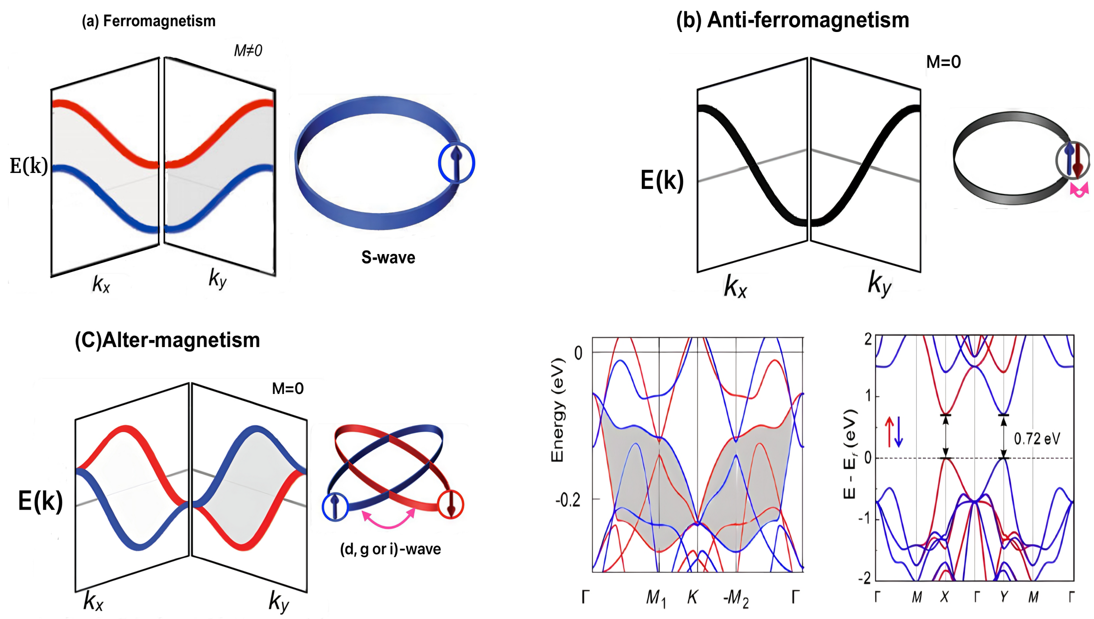

Figure 1.1: In this figure, blue and red colours are used for depicting opposite spin directions, adapted from Ref.[1] (a) Momentum independent spin-splitting of bands in ferromagnets , Isotropic s-wave spin-split fermi surfaces. (c) A model of altermagnetism where Opposite spin lattices are connected by rotation symmetry, time reversal symmetry breaking spin splitting, anisotropic d-wave spin-split fermi surfaces. (d)Spin-split band structure of Mn_5Si_3(left) and V_2Se_2O(right) taken from Ref.[2, 3].

The identification of this phase as a distinct magnetic phase is favoured by delimitising the unconventional magnetic phase of high even parity wave (or the d-wave) form as a different symmetry type. We use a symmetry approach based on non-relativistic spin-group formalism [5, 6] to derive distinct phases of non-relativistic collinear magnetism [4].

In first phase it has been found that there is either only one spin lattice or opposite spin sublattices not connected by any symmetry transformations(i.e conventional ferrromagnetism or ferrimagnetism)[7]. In the second phase, opposite-spin sublattices are connected by inversion or translation or both which coresponds to conventional antiferromagnetism[8] and the third phase has opposite-spin sublattices not connected by inversion or translation but connected by rotation . Unlike the two phases the third phase has equally polulated spin-up and spin-down energy isosurfaces that break time reversal symmetry i.e the spin-group symmetries protect zero net magnetisation and simultaneously allow for the spin-split $\mathcal{T}$-symmetry broken electronic band structure.[4]

Spin groups exhibit both the symmetries, those which are common to collinear magnetic phases(spin-only groups) and those which corresponds exclusive to one of the three magnetic phases(non-trivial spin groups).In Table1.1 we highlight the spin-group symmetries with correspondind crystal structure and non-relativistic band structure characterstics for altermagnets.

Spin-group symmetries	Crystal structure	Non-relativistic Band structure
$[E\|\|H][\mathrm{C}_2$——AH]	spin-density anisotropy in sublattices	Spin-Fermi-surface anisotropy
$[C_2\|\|AH]$	Compensated	$\mathcal{T}$-symmetry breaking, spin splitting at general k
$L_k \cap AH \neq \Phi$		Spin degeneracy at high symmetry k

Table 1.1: Three lines regard symmetries apply to altermagnets.The table is adopted from Ref.[4]

The spin groups that describe the electronic structure of conventional ferromagnetic phase , conventional antiferromagnetic phase and those which are exclusively specific to the non-relativistic energy bands of altermagnets are respectively given by [4]-

$$R_s^I = [E||G] \tag{1.1}$$

$$R_s^{II} = [E||G] + [C_2||G] \tag{1.2}$$

$$R_s^{III} = [E||H] + [C_2||AH] \tag{1.3}$$

Where R_s^{III} represents ten spin Laue groups describing altermagnets , E denotes spin-space identity transformation, G is the nonmagnetic crystallographic group with H as it's subgroup having half of the real space transformations of group **G**. A Schemetic of above discussion is shown in Fig 1.2, where the opposite spin-sublattice transforation of the spin-Laue group mapping the eigenstates of same energy with opposite spins on the same k-vector in second magnetic phase and on different k-vectors in the third magnetic phase is highlighed.

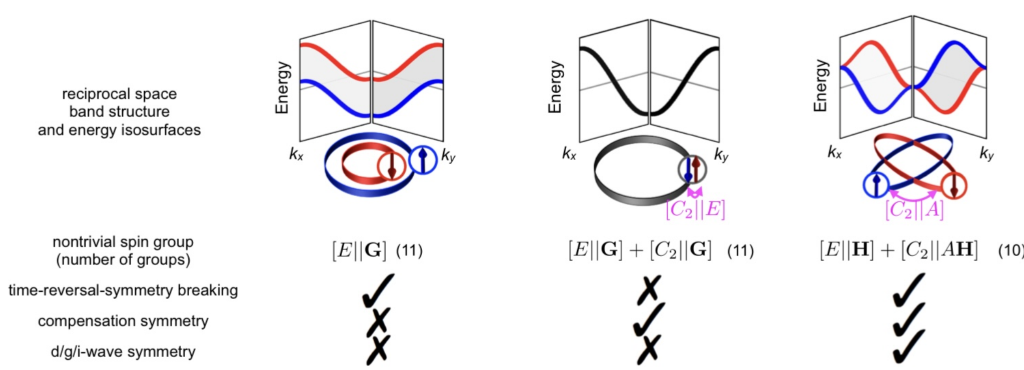

Figure 1.2: The last three rows showing the spin-Laue group structure for all the three magnetic phase with the number of different groups in brackets. The presence of $\mathcal{T}$-symmetry breaking, compensation symmetry and spin-wave symmetries is shown for given phases.Figure is taken from [4].

1.2 Tight Binding model Hamiltonian

To find a Hamiltonian describing spin-split band structure in altermagnets, We proceed by considering a quasi two dimensional altermagnetic lattice which is depicted in figure 1.3(a). A schematic of such a tight binding model of spin d-wave interaction is shown in figure 1.4(b) where kinetic nearest neighbour hopping is parameterized by t and alternating spin-momentum coupling by a spin-dependent parameter t_j.

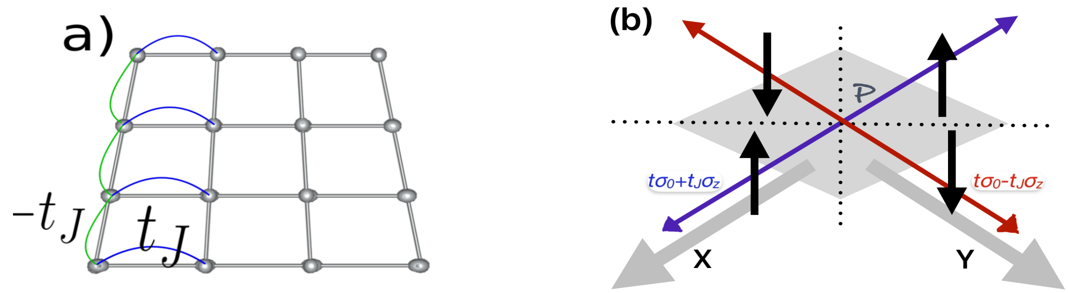

Figure 1.3: (a) A Schemetic of 2D lattice is presented, t_j takes opposite signs in x and y directions.(b)A representation of the kinetic nearest hopping with spin-dependent hopping about the inversion centre $\mathcal{P}$. Figure is adapted from [2]

In this tight binding model we consider only one quantum state for each spin. The creation (annihilation) operator $c_i^{+}(c_i)$ creates and annihilates one particle on site "i". In the Hamiltonian, the first term is to be taken for the kinetic nearest-neighbor hopping and the second term for the unconventional d-wave Zeeman interaction due to the Coulomb-exchange dependent hopping. Physically, this term can be understood as an exchange molecular field that is felt by the electron when it hops on top of the collinear antiferromagnetic-background. The sign of the exchange dependent hopping is positive along the x-axis and negative along the y-axis . The non-interacting Hamiltonian can thus be written as-

$$H = -t \sum_{\langle i,j \rangle} (C_i^{\sigma\dagger} C_j^{\sigma} + C_j^{\sigma\dagger} C_i^{\sigma}) - t_j \sum_{\langle i,j \rangle, \sigma' \neq \sigma} (C_i^{\sigma'\dagger} C_j^{\sigma} + C_j^{\sigma\dagger} C_i^{\sigma'}) \tag{1.4}$$

where $\langle i,j \rangle$ means i and j must be nearest neighbours.

Since $C_i^{\sigma\dagger} C_j^{\sigma}$ and $C_j^{\sigma\dagger} C_i^{\sigma}$ are complex conjugate to each other we can write-

$$H = -t \sum_{\langle i,j \rangle} (C_i^{\sigma\dagger} C_j^{\sigma}) - t_j \sum_{\langle i,j \rangle, \sigma' \neq \sigma} (C_i^{\sigma'\dagger} C_j^{\sigma}) + h.c \tag{1.5}$$

With $h.c$ denoting the hermitian conjugate of previous terms. Since we are considering hopping in x-y plane shown in figure(2) above we will consider two unit vectors j_1 and j_2 in the direction of hopping -

$$\vec{j_1} = (1,0), \vec{j_2} = (0,1) \tag{1.6}$$

Moreover from figure 3(b) it is evident that the spin orbit interaction term t_j has opposite signs in x and y directions so considering that and introducing vectors j_1 and j_2 in previous equation we get

$$H = -t \sum_i C_i^{\sigma\dagger} C_{i+j_1}^{\sigma} - t \sum_i C_i^{\sigma\dagger} C_{i+j_2}^{\sigma} + t_j \sum_{i\sigma' \neq \sigma} C_i^{\sigma'\dagger} C_{i+j_1}^{\sigma} - t_j \sum_{i\sigma' \neq \sigma} C_i^{\sigma'\dagger} C_{i+j_2}^{\sigma} + h.c \tag{1.7}$$

If we go to the momentum space by performing 2-D fourier transformation we obtain-

$$C_i^{\sigma} = 1/\sqrt{N} \sum_k a_k \exp\left\{-i\vec{k} \cdot \vec{r}\right\} \tag{1.8}$$

using equation (5) the first term of hamiltonian in momentum space is found to be -

$$-t \sum_i C_i^{\sigma\dagger} C_{i+j_1}^{\sigma} = \frac{-t}{N} \sum_{k,k'} a_k^{\sigma\dagger} a_{k'}^{\sigma} e^{i(k-k')\cdot\vec{r}} e^{(-ik'\cdot j_1)} \tag{1.9}$$

thus further solving eqn(4) using eqn(6)

$$\begin{aligned}
H = \frac{1}{N} [& -t \sum_{i,k,k'} a_k^{\sigma\dagger} a_{k'}^{\sigma} e^{i(k-k')\cdot\vec{r}} e^{(-ik'\cdot j_1)} - t \sum_{i,k,k'} a_k^{\sigma\dagger} a_{k'}^{\sigma} e^{i(k-k')\cdot\vec{r}} e^{(ik'\cdot j_1)} \\
& -t \sum_{i,k,k'} a_k^{\sigma\dagger} a_{k'}^{\sigma} e^{i(k-k')\cdot\vec{r}} e^{(-ik'\cdot j_2)} - t \sum_{i,k,k'} a_k^{\sigma\dagger} a_{k'}^{\sigma} e^{i(k-k')\cdot\vec{r}} e^{(ik'\cdot j_2)} \\
& +t_j \sum_{i,k,k'} a_k^{\sigma\dagger} a_{k'}^{\sigma} e^{i(k-k')\cdot\vec{r}} e^{(-ik'\cdot j_1)} + t_j \sum_{i,k,k'} a_k^{\sigma\dagger} a_{k'}^{\sigma} e^{i(k-k')\cdot\vec{r}} e^{(ik'\cdot j_1)} \\
& -t_j \sum_{i,k,k'} a_k^{\sigma\dagger} a_{k'}^{\sigma} e^{i(k-k')\cdot\vec{r}} e^{(-ik'\cdot j_2)} - t_j \sum_{i,k,k'} a_k^{\sigma\dagger} a_{k'}^{\sigma} e^{i(k-k')\cdot\vec{r}} e^{(ik'\cdot j_2)}]
\end{aligned} \tag{1.10}$$

Using $\frac{1}{N}\sum_i e^{i(k-\vec{k'}).\vec{r_i}} = \delta_{k,k'}$

$$H = -t\sum_k a_k^{\sigma\dagger} a_k^{\sigma}(e^{-ik_x} + e^{ik_x}) - t\sum_k a_k^{\sigma\dagger} a_k^{\sigma}(e^{-ik_y} + e^{ik_y})$$
$$-t_j\sum_k a_k^{\sigma\dagger} a_k^{\sigma}(e^{-ik_x} + e^{ik_x}) + t_j\sum_k a_k^{\sigma\dagger} a_k^{\sigma}(e^{-ik_y} + e^{ik_y}) \tag{1.11}$$

we have to consider two different operators for up spin and down- spin ,taking them as $c_k^{\dagger\uparrow}(c_k^{\uparrow})$ and $c_k^{\dagger\downarrow}(c_k^{\downarrow})$ respectively and writing the Hamiltonian given in eqn (8) in matrix form we get -

$$H = \begin{pmatrix} c_k^{\dagger\uparrow} & c_k^{\dagger\downarrow} \end{pmatrix} \begin{pmatrix} t(\cos k_x + \cos k_y) & t_j(\cos k_x - \cos k_y) \\ t_j(\cos k_x - \cos k_y) & t(\cos k_x + \cos k_y) \end{pmatrix} \begin{pmatrix} c_k^{\uparrow} \\ c_k^{\downarrow} \end{pmatrix} \tag{1.12}$$

The kernel of above hamiltonian gives the expression of Hamiltonian and the dispersion relation for altermagnetic system. Denoting $(\cos k_x + \cos k_y)$ by $\mathcal{A}$ and $(\cos k_x - \cos k_y)$ by $\mathcal{B}$, the kernel of hamiltonian reads.

$$H(k) = \begin{pmatrix} t\mathcal{A} & t_j\mathcal{B} \\ t_j\mathcal{B} & t\mathcal{A} \end{pmatrix} \tag{1.13}$$

Now, diagonalizing the matrix (1.13) we obtain-

$$H(k) = \begin{pmatrix} t\mathcal{A} + t_j\mathcal{B} & 0 \\ 0 & t\mathcal{A} - t_j\mathcal{B} \end{pmatrix}$$

The Hamiltonian describes a magnetic lattice shown in Fig. Considering a unit vector d along the N´eel , vector 1 ss the unit matrix and σ as the vector of Pauli spin matrices, We can write the Hamiltonian for altermagnetic system in more general and simlified form as-

$$\boxed{H(k) = 2[t(\cos k_x + \cos k_y) \cdot \mathbf{1} + t_j(\cos k_x - \cos k_y)\sigma \cdot d]} \tag{1.14}$$

From Eqn[1.14], the spin-up and spin-down energy bands are given by-

$$E_s(k) = 2t(\cos k_x + \cos k_y) + s\ 2t_j(\cos k_x - \cos k_y) \tag{1.15}$$

With s representing $\pm$ sign. The anisotropic spin-momentum coupling shown in figure (1.4) is obtained by performing $k \cdot p$ approximation around the τ point taking Eqn[1.15] into account, the energy spectrum can now be written as

$$E_s(k) = 4t - (t \pm t_j)k_x^2 - (t \mp t_j)k_y^2 \tag{1.16}$$

On the other hand, valley dependent spin-momentum coupling is obtained from Eq. (1.15) by performing the $k \cdot p$ approximation in M1 and M2 valleys. In this case the dispersion relation is

$$E_s(M_1, k) = st_j(4 - k^2)$$
$$E_s(M_2, k) = -st_j(4 - k^2) \tag{1.17}$$

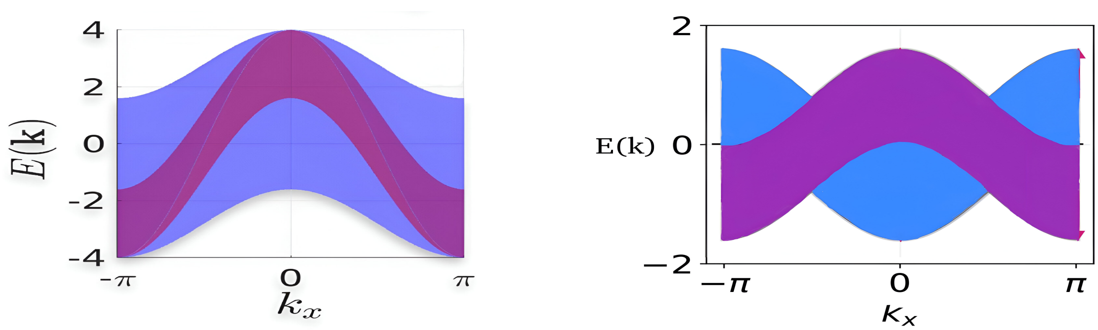

Figure 1.4: Spin-up and spin-down (violet and blue) energy bands as the function of k_x plotted for the discrete transverse parameters.Energy ranges with separated spin-up and spin-down channels due to the presence of the spin-polarized valleys.

1.3 Time reversal symmetry breaking from antiferromagnetic Zeeman effect.

Spin polarization by the $\mathcal{T}$-symmetry breaking can be seen microscopically if we probe on an individual atom of antiferromagnets [9]but on the macroscopic level, it was assumed that the effect cancels out due to antiparallel allignment of the local Coulomb-exchange fields on the neighbouring atoms. However, the band structure shown in Fig.(1.4) obtained by model Hamiltonian (1.14) near M1 and M2 valleys shows the antiferromagnetic zeeman interaction of the electron's spin with the field, the zeeman field is opposite in the M1 and M2 valleys and couples only to the z component of spin, as highlighted in Fig.[1.5a][2].

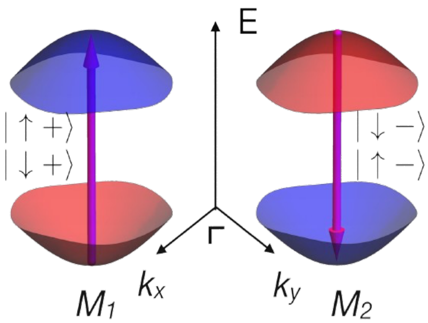

(a)

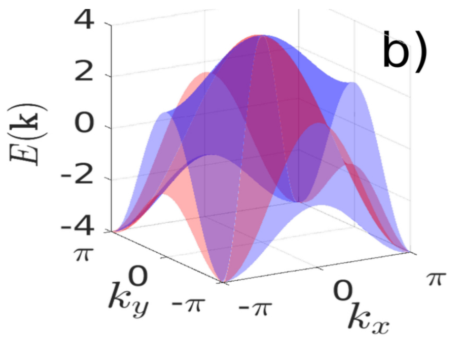

(b)

Figure 1.5: (a) Antiferromagnetic Zeeman effect with opposite zeeman field shown by magneta arrows arround M_1 and M_2 valleys.Blue and red bands corresponds to the spin-up and down polarization respectively. (b) Energy Bands over the full Brillouin zone from Zeeman Hamiltonian.

If we draw the energy bands of Hamiltonian over the full Brillouin zone [Fig-1.5b],it highlights the coexistence of the Macroscopic spontaneous $\mathcal{T}$-symmetry breaking with the zero net moment and preserved p-symmetry[2].The spontaneous Hall effect has been experimentally measured in Mn_5Si_3 epilayers to demostrate the time-reversal symmetry breaking in Zeeman-split antiferromagnet and the experimental Hall conductivities are found to be consistent with ab initio band structure calculations[2].Beside 3D crystals, the spin-split valleys can also form in 2D materials [10, 11]

1.4 Anomalous Hall effect in Altermagnets

The time-reversal symmetry breaking is responsible for the dissipationless Hall current. When it is ascribed to spontaneous non-zero total internal magnetization the effect is called anomalous Hall effect. Theoretical predictions and experimental observations have identified such large Hall effects in altermagnets. In order to find the Hamiltonian that is able to describe this phenomenon, we have to look into the related physical concepts more deeply.

1.4.1 Berry phase and Band topology

Berry's phase is defined as a response of quantum mechanical system to an infinitely slow variation of the Background variable. Berry curvature and Berry connection are related concepts with berry phase that has been of tremendous importance in condensed mater theory giving rise to intresting phenomenas like anomalous Hall effect and negative magnetoresistence .In crystal momentum space the Berry connection is analogous to the electrodynamic vector potential and Berry curvature is analogous to the Magnetic field.

If $A_n(k)$ represents Berry connection , $B_n(k)$ - Berry curvature and u_{nk} is the periodic part of Bloch function, we can write-

$$\begin{aligned} A_n(k) &= i\langle u_{nk}|\Delta_k u_{nk}\rangle \\ B_n(k) &= \Delta_k \times A_n(k) \end{aligned} \tag{1.18}$$

In time-reversal symmetry broken or space- inversion symmetry broken systems , the non-zero Berry curvature can generate anomalous velocity that is transverse to the applied electric field and thus give rise to the anomalous transport currents, making an intrinsic contribution to Hall conductivity[12, 13].We can write the kubo formula for Transverse conductivity in terms of Berry phase .

$$\sigma_{xy} = -\frac{e^2}{\hbar}\sum_n \int_{BZ} \frac{d^3k}{(2\pi)^3}\, f[\epsilon_n(k)]B_n^z(k) \tag{1.19}$$

Eqn.[1.18, 1.19] show direct connection between Hall effect and concept of geometrical Berry phase. Since, time-reversal operator is anti-unitary in Quantum mechanics the Berry curvature (Eqn.24) is odd under time-reversal i.e $TB_n(k) = -B_n(-k)$, this emplies that in $\mathcal{T}$-symmetric Band structures the integral (Eqn.24) vanishes and hence no macroscopic Hall effect is visible. Thus, the breaking of time-reversal symmetry in the Band structures is the key requirement for the observation of macroscopic responses such as anomalous Hall conductivity.

The role of topology- The Berry-phase concept has also been successful in establishing link between the anomalous hall effect and topological nature of the Hall currents with experimental varifications. In fact both the integer and fractional QHE's can be explained in terms of topological properties of the electronic wave-functions. In 2-D crystals it has been found that the Hall conductance is connected by Chern number defined for the Bloch wave function over the first Brillouin zone[14] .

$$\sigma_{xy} = -\frac{e^2}{2\pi h}C \tag{1.20}$$

Here C is what is known as first Chern number, it is obtined by integrating the curvature over the brillouin zone .The relationship between the Hall conductivity and the Chern number is usually referred to as the TKNN invariant.The TKNN formula is the statement that the Hall conductivity is a topological invariant of the system.

1.4.2 Role of Rashba Spin-orbit coupling

The Rashba effect is a momentum-dependent splitting of spin bands in low-dimensional condensed matter systems (such as Heterostructures and surface states).In heterostructures the conduction band discontinuity give rise to a internal potential gradient and so the strong electric field which interacts with the quasi-free electron in the conduction band, this interaction is referred to as Rashba interaction or spin-orbit interaction due to structural inversion asymmetry (since the internal electric field give rise to the SIA in conduction band profile).

Here we present a systimatic approach to arrive at the Rashba Hamiltonian by considering the spin-orbit coupling in relativistic viewpoint. For this we take electron's frame of reference where the nucleous is revolving around electron with speed v and generating a magnetic field $\vec{B}$ at the centre. We'll consider the magnetic field in terms of the potential gradient(or electric field) using well known electrodynamic relation so that the formalism could be generally valid for any intrinsic electric field . If $\vec{E}$ is the Electric field of nucleous then the magnetic field for this system can be written as-

$$B = \frac{\vec{E} \times \vec{v}}{c^2}$$

Implying 2-factor correction done by Rasba the modified expression for magnetic field becomes-

$$B = \frac{1}{2}\frac{\vec{E} \times \vec{v}}{c^2} \tag{1.21}$$

the relativistic version of this equation takes the form-

$$B = \frac{\vec{E} \times \vec{v}}{2c^2\sqrt{1-\frac{v^2}{c^2}}} \tag{1.22}$$

We know that, for an electron with spin s interacting with magnetic field $\vec{B}$, spin-orbit interaction energy is given by-

$$E_r = g_0 \mu_B \vec{s} \cdot \vec{B} \tag{1.23}$$

where g denotes Landau's g-factor and μ_B is Bohr magnaton as usual. Using equation (20) by considering that $\mu_B = \frac{e\hbar}{2m}$ and $\vec{s} = \frac{\sigma}{2}$, spin-orbit energy now can be written as -

$$E_r = \frac{g_o e\hbar}{4m}\frac{\vec{E} \times \vec{v}}{2c^2\sqrt{1-\frac{v^2}{c^2}}} \cdot \vec{\sigma} \tag{1.24}$$

As $E = -\nabla\vec{v}$, for electron $g_o = 2$.

$$E_r = \frac{-e\hbar}{4m^2c^2\sqrt{1-\frac{v^2}{c^2}}}(\nabla\vec{v} \times \vec{p}) \cdot \vec{\sigma} \tag{1.25}$$

An electron in a solid behaves like a free quasiparticle with reduced mass m^* ,thus pin-orbit interaction Hamiltonian for electron in a solid can be written as-

$$H_0 = \frac{ge\hbar}{8m^*c^2\sqrt{1-\frac{v^2}{c^2}}}\nabla\vec{v}\cdot(\vec{\sigma}\times\vec{p}) \tag{1.26}$$

for electrons moving in crystals with speed much smaller than the speed of light we can ommit the relativistic factor and get-

$$\boxed{H_0 = \frac{ge\hbar}{8m^*c^2}\nabla\vec{v}\cdot(\vec{\sigma}\times\vec{p})} \tag{1.27}$$

The Rashba Hamiltonian can be obtained from Eqn (25) in straighforward way, the form of Hamiltonian is nothing but 2-D version of Dirac Hamiltonian.

$$\boxed{H = \lambda\hat{z}\cdot(\vec{\sigma}\times\vec{p})} \tag{1.28}$$

Where is the Rashba coupling term and $\hat{z}$ is the unit vector along the direction of the electric field.

When the Rashba spin-orbit iteraction is introduced to generate an (anti)crossing at the Γ-point in metallic ferromagnets, it results in band splitting with strongly peaked Berry curvature at the anticrossing. The 2D model Hamiltonian for such systems requires the contribution of Rashba spin-orbit coupling term which we have just now derived. When we plot the Berry curvature for such a system a large Hall-conductance can arise from a Berry curvature strongly peaked at anti(crossing). If we emply the same model to arrive at Berry phase phenomenology in altermagnets we get anisotropic Berry curvature around Γ-point band crossing[15].

1.5 Total Hamiltonian

In order to realise the large Berry curvature observed in altermagnetic candidates [16, 17, 18], a 2-D Hamiltonian representing the ground state of the system is needed (a 2D Hamiltonian can represent altermagnetic system because in spin-group formalism this model corresponds to 2D non-relativistic spin symmetry group which allows the rotation transformations with inversion or translation transformtion, identifying this third phase theoretically). If we consider our previous discussions to account for the experimental evidences of large Berry phase, a general hamiltonian should include the kinetic energy term, a term explaining spin-splitting and spin-orbit interaction term responsible for Hall conductivity. We know that the $k \cdot p$ models has been useful to analytically calculate the physical properties of materials like non-trivial topologies and novel response to various external fields. The K.p approximation focuses on the behaviour of electrons near the band edge, typically at high symmetry points. Thus the 2D Hamiltonian is being considered under k.p altermagnet-Rashba model which is given by

$$H = tk^2 + 2t_j \sigma_z k_x k_y + \lambda(\sigma_y k_x - \sigma_x k_y). \tag{1.29}$$

Where the first two term is taken from Eqn[1.14] and the third term for is taken from Eqn[1.28] denoting the rashba spin-orbit interaction in altermagnets.

CHAPTER 2

Formulation of Optical conductivity tensor

2.1 Kubo formula for Hall conductivity

The formula that relates Hall conductivity to the quantum mechnical variables is called Kubo formula and it is the part of a more genaral theory called *leniar response theory*. If you apply an electric field at frequency Ω, the current responds by oscillating at the same frequency, this is what we mean by "the linear response". If a 2D system is exposed to an electric field of momentum $\mathbf{k}$ and frequency Ω, the current density is given by

$$J_\alpha(r,t) = \sum_\beta \sigma_{\alpha\beta}(k,\Omega) E_\beta \exp\{i(k.r) - \Omega t\} \tag{2.1}$$

where $J_\alpha(r,t)$ is electric current and $E_\beta \exp\{i(k.r) - \Omega t\}$ is the electric field. If we define the current in terms of the group velocity of the wavepackets, i.e $J = \frac{e}{\hbar}\frac{\partial H}{\partial k}$, where H is the Hamiltonian, Kubo formula for Hall conductivity reads-

$$\sigma_{xy} = \frac{ie^2}{\hbar(2\pi)^2} \times$$
$$\sum_{E_\beta < E < E_\alpha} \int_{BZ} d^2k \, \frac{\left\langle u_k^\alpha \middle| \partial_y H \middle| u_k^\beta \right\rangle \left\langle u_k^\beta \middle| \partial_x H \middle| u_k^\alpha \right\rangle - \left\langle u_k^\alpha \middle| \partial_x H \middle| u_k^\beta \right\rangle \left\langle u_k^\beta \middle| \partial_y H \middle| u_k^\alpha \right\rangle}{(E_k^\beta - E_k^\alpha)^2} \tag{2.2}$$

Where Integration is done over Brillouin zone, momentum is represented by "k" and index α and β runs over filled bands and empty bands respectively.

For studying the AHE theoretically it is best to reformulate kubo formula for optical conductivity in the form of Bastin Formula because it only requires the variables that can be calculated if we know the Hamiltonian of the system under study .This formula is interesting because it expresses the conductivity as a product of velocities and Green's functions[19]. Thus in Matsubara formalism the expression for the conductivity tensor takes the form

$$\sigma_{\alpha\beta}(k, \Omega_n) = \frac{ie^2}{\hbar 4\pi^2 \Omega} \int_{BZ} d^2k \, T \sum_{k,\Omega_l} Tr\langle v_\alpha(k) G[k, i\Omega_l)] v_\beta(k) G[k, i(\Omega_n + \Omega_l)]\rangle \tag{2.3}$$

with frequencies $\Omega_n = \frac{2n\pi}{\beta}$ and $\Omega_l = \frac{(2l+1)\pi}{\beta}$. These frequencies are called Bosonic and fermionic frequancies respectively. The Matsubara Green function in the above expression is given by

$$G(k, i\Omega_n) = [i\Omega_n - H(k)]^{-1} \tag{2.4}$$

Further we use the method of analytical continuation by taking $i\Omega_l = \Omega + i\delta$ and $\delta \to 0$,finally eqn (26)is given by

$$\sigma_{\alpha\beta} = i\frac{e^2}{\hbar 4\pi^2 \Omega} \lim_{\delta \to 0} \int_{BZ} d^2k \, T \sum_{k,\Omega_l} Tr\langle v_\alpha(k) G[k, \Omega_l)] v_\beta(k) G[k, \Omega_n + \Omega_l]\rangle_{i\Omega \to \Omega + i\delta} \tag{2.5}$$

Expanding the matsubara green functions in matrix form we can get above equation in more simplified form.

$$\sigma_{\alpha\beta} = i\frac{e^2}{4\hbar 4\pi^2\Omega}\lim_{\delta\to 0}\int_{BZ} d^2k \sum_k \mathrm{Tr}\left[v_\alpha(\mathbf{k})\begin{pmatrix} G_{11} & G_{12} \\ G_{21} & G_{22}\end{pmatrix} v_\beta(\mathbf{k})\begin{pmatrix} G_{11} & G_{12} \\ G_{21} & G_{22}\end{pmatrix}\right]$$
$$\times \sum_l G_0^s(\mathbf{k},\Omega_l)G_0^{s'}(\mathbf{k},\Omega_l+\Omega_n)|_{i\Omega_n\to\Omega+i\delta} \quad (2.6)$$

2.2 Matsubara frequency summation

To proceed further with the solution of conductivity tensor, the summation part of the Eqn [2.16] needs to be countered. Here we present a detailed Summation formalism using the method of analytical continuation for summation of Matsubara frequencies. To evaluate the summation over ($l \in \mathbb{Z}$) in eqn(2.16), we denote-

$$I^n_{s,s'}(\mathbf{k}) = \sum_l G_0^s(\mathbf{k},\Omega_l)G_0^{s'}(\mathbf{k},\Omega_l+\Omega_n)$$
$$= \sum_l \frac{1}{\mu + i\Omega_l - E_s(\mathbf{k})}\frac{1}{\mu + i(\Omega_l+\Omega_n) - E_{s'}(\mathbf{k})}. \quad (2.7)$$

Here $E_s(\mathbf{k})$ is the resulting bands of the given physical system. Consider the integral $\oint_C \frac{f(z)}{[z-E_s(\mathbf{k})][z+i\Omega_n-E_s'(\mathbf{k})]}$ to be integrated over the closed contour as shown in Fig. [2.1]. Using the Cauchy's residue theorem, one can arrive at the following equation[**?**].

$$\oint_C \frac{f(z)}{[z-E_s(\mathbf{k})][z+i\Omega_n-E_s'(\mathbf{k})]}$$
$$= 2\pi i\sum_l \mathrm{Res}\Big[\frac{f(z)}{[z-E_s(\mathbf{k})][z+i\Omega_n-E_{s'}(\mathbf{k})]}\Big]_{z=i\Omega_l} \quad (2.8)$$

where $z = i\Omega_l = i\pi(2l+1)/\beta$ are the pole of the Fermi-Dirac distribution function $f(z)$. The residue on the RHS of the above integral is

$$\mathrm{Res}\Big[\frac{f(z)}{[z-E_s(\mathbf{k})][z+i\Omega_n-E_{s'}(\mathbf{k})]}\Big]_{z=i\Omega_l}$$
$$= -\frac{1}{\beta}\frac{1}{\mu+i\Omega_l-E_s(\mathbf{k})}\frac{1}{\mu+i(\Omega_l+\Omega_n)-E_{s'}(\mathbf{k})}. \quad (2.9)$$

The summation over l can be thus written as (from Eqn[2.9],[2.8] and [2.7])

$$\sum_l I_{s,s'}(\mathbf{k}) = -\frac{\beta}{2\pi i}\oint_C f(z)\frac{1}{[z - E_s(\mathbf{k})][z + i\Omega_n - E'_s(\mathbf{k})]} \tag{2.10}$$

Using the above results, the summation can be written as

$$\begin{aligned} &\textstyle\sum_{l\in\mathbb{Z}} \mathrm{Tr}[\hat{v}_\mu(\mathbf{k})\hat{G}(\mathbf{k},\Omega_l)\hat{v}_\mu(\mathbf{k})\hat{G}(\mathbf{k},\Omega_l+\Omega_n)] \\ &= -\mathcal{F}_\chi(\mathbf{k})\textstyle\sum_{s\neq s'} \frac{\beta}{2\pi i}\oint_C f(z)\frac{1}{[z-E_s(\mathbf{k})][z+i\Omega_n-E_{s'}(\mathbf{k})]} \end{aligned} \tag{2.11}$$

We notice that the integral on the RHS in the above Eq. has branch cuts along the real axis $\mathrm{Im}[z] = 0$ and along $\mathrm{Im}[z] = -i\Omega_n$. In order to evaluate the integral

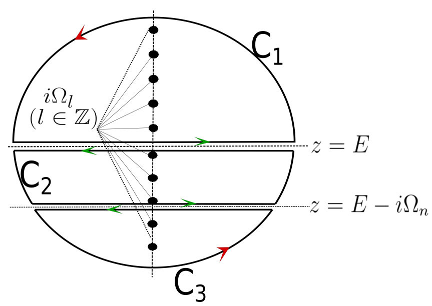

Figure 2.1: The different contours for the complex Matsubara frequency summation: The horizontal lines $\mathrm{Im}(z) = 0$ and $\mathrm{Im}(z) = -i\Omega_n$ denote the two branch cuts in the complex plane. The three contours of integration C_1, C_2, and C_3. The dots about the imaginary axis gives the poles of the Fermi-Dirac distribution function $f(z)$.

on the right hand side of the above Eq. [2.11], we modify the contour to be a sum of the closed paths C_1, C_2, and C_3 in order to avoid the two mentioned brancuts (refer to Fig. [2.1]). By extending the contour to infinity, the integral in Eq. [2.11] can be evaluated about the horizontal paths (shown by the green arrows). Thus we can change the integration variable to $z = E + i\eta$ for C_1, ($z = E - i\eta$ and $z = E - i\Omega_n + i\eta$ about the two horizontal lines in C_2) and $z = E - i\Omega_n - i\eta$

for C_3, where $\eta \to 0$ is a positive infinitesimal number. After some amount of calculus, we then obtain

$$\oint_C \frac{f(z)dz}{[z - E_s(\mathbf{k})][z + i\Omega_n - E_{s'}(\mathbf{k})]} = 2\pi i \frac{f[E_{s'}(\mathbf{k})] - f[E_s(\mathbf{k})]}{E_s(\mathbf{k}) + i\Omega_n - E_{s'}(\mathbf{k})} \quad (2.12)$$

Using the above results we finally have

$$\begin{aligned} &\textstyle\sum_{l\in\mathbb{Z}} \mathrm{Tr}[\hat{v}_\mu(\mathbf{k})\hat{G}(\mathbf{k},\Omega_l)\hat{v}_\mu(\mathbf{k})\hat{G}(\mathbf{k},\Omega_l+\Omega_n)] \\ &= -\beta\mathcal{F}_\chi(\mathbf{k}) \textstyle\sum_{s\neq s'} \frac{f[E_{s'}(\mathbf{k})]-f[E_s(\mathbf{k})]}{E_s(\mathbf{k})+i\Omega_n-E_{s'}(\mathbf{k})}. \end{aligned} \quad (2.13)$$

Thus, after the general solution of the conductivity tensor represented by Eqn.[2.16] takes the form

$$\begin{aligned} \sigma_{\alpha\beta} \quad &= i\frac{e^2}{4\hbar 4\pi^2\Omega} \lim_{\delta\to 0} \sum_{s\neq s'} \int_{BZ} d^2k \sum_k \mathrm{Tr}\left[v_\alpha(k)\begin{pmatrix} G_{11} & G_{12} \\ G_{21} & G_{22}\end{pmatrix} v_\beta(k)\begin{pmatrix} G_{11} & G_{12} \\ G_{21} & G_{22}\end{pmatrix}\right] \\ &\times \frac{f[E_{s'}(\mathbf{k})] - f[E_s(\mathbf{k})]}{E_s(\mathbf{k}) + \Omega + i\delta - E_{s'}(\mathbf{k})} \end{aligned} \quad (2.14)$$

Where f(x) represents the fermi-distribution and the values of matrix elements are to be determined by the Hamiltonian of the corresponding system. To extract the physical properties of the said system the real and imaginary part of the solution is to be found.

CHAPTER 3

Calculations and Result

3.1 Ground state of altermagnets

The Hamiltonian that gives the said ground state of the altermagnetic system with unique Berry phase phenomena is given by

$$H = t_0\sigma_0 k^2 + 2t_j\sigma_z k_x k_y + \lambda(\sigma_y k_x - \sigma_x k_y). \tag{3.1}$$

Here we have parametrized the kinetic nearest-neighbor hopping by t_0, the alternating spin-momentum coupling by a spin-dependent hopping parametrized by t_j and λ is the magnitude of the Rashba spin-orbit coupling. We also defined $\boldsymbol{\sigma} = (\sigma_x, \sigma_y, \sigma_z)$ to be the usual Pauli's matrices and σ_0 the 2×2 identity matrix. The two-level energy dispersion of the Hamiltonian Eqn(3.1) are -

$$E_s = k^2 t + s\sqrt{\lambda^2 k^2 + k^4 tj^2 sin^2(2\theta)} \tag{3.2}$$

Here in the second term, $s = +/-$ denoting the two spin-split states and the remaining term $\sqrt{\lambda^2 k^2 + k^4 tj^2 sin^2(2\theta)}$ is to be denoted by Δ_k the anisotropic spin-splitting between contributed by the quantity t_j.

The corresponding eigen spinors of the spin-split dispersion are given as

$$\psi_+(\mathbf{k}) = \begin{pmatrix} \cos\frac{\xi_{\mathbf{k}}}{2} \\ i\sin\frac{\xi_{\mathbf{k}}}{2}e^{i\phi_{\mathbf{k}}} \end{pmatrix} \text{ and} \tag{3.3}$$

$$\psi_-(\mathbf{k}) = \begin{pmatrix} \sin\frac{\xi_{\mathbf{k}}}{2} \\ -i\cos\frac{\xi_{\mathbf{k}}}{2}e^{i\phi_{\mathbf{k}}} \end{pmatrix}, \tag{3.4}$$

where $\xi_{\mathbf{k}} = \arccos[\frac{t_j k^2 \sin 2\phi_{\mathbf{k}}}{\Delta_{\mathbf{k}}}]$.

We now define the spin-vector of the two spin-split states as $\mathbf{S}^s = \{S_x^s, S_y^s, S_z^s\}$, where $S_\nu^s = \hbar/2\langle s, \mathbf{k}|\sigma_\nu|s, \mathbf{k}\rangle$. The form of each component is given below

$$\begin{pmatrix} S_x^s \\ S_y^s \\ S_z^s \end{pmatrix} = \frac{\hbar}{2}\begin{pmatrix} -s\sin\phi_{\mathbf{k}}\sin\xi_{\mathbf{k}} \\ s\cos\phi_{\mathbf{k}}\sin\xi_{\mathbf{k}} \\ s\cos\xi_{\mathbf{k}} \end{pmatrix} \tag{3.5}$$

thus giving a spin-momentum locking phenomenon, i.e. $\mathbf{S}^s \cdot \mathbf{k} = 0$. We show the plots of the spectrum from Eq. [45] in Fig. [7(a)] attched to it with a spin configuration resulting from Eq. [48] at a given constant energy.

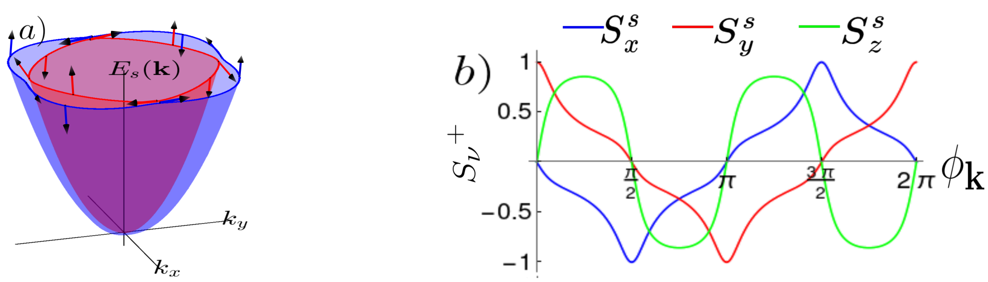

Figure 3.1: a) The schematic of the dispersion from Eq. [3.2]. The two types of arrows show the orientation of the vectors in Eq. [3.5] about a constant energy contour. b) Plots of the vector $\mathbf{S}_\nu^+$ (in units of $\hbar/2$) vs $\phi_{\mathbf{k}}$ over each point of the constant energy contours (E_+ & E_-).

It is important to note that there is minimum SOC splitting along the azimurthal directions $\phi_{\mathbf{k}} = n\pi/2$ (n being an integer) (where the two spin vectors are tangential to the (k_x, k_y) plane), whereas the same is maximum about the directions $\phi_{\mathbf{k}} = (2n+1)\pi/4$ (where the S_z^s component of the two spin vectors is maximum). The above property is what set it apart from the relativistic Rashba spin-split bands.

3.2 Calculation of the optical conductivity tensor

The typical value of the different parameters that we will consider for calculations is shown in the table 3.1, below.

Parameters	(in arbitrary units)
t_0	$\frac{\hbar^2}{2m^*}$
t_j	$0.4\ t_0$
λ	5×10^{-11} eV m

Table 3.1: Taking $m^* = 0.05\ m_0$, with m_0 being the bare electron mass.

Now, we start with the Kubo formula for optical conductivity to calculate σ_{xx} and σ_{yy}, where

$$\sigma_{xx}(\Omega) = \lim_{\delta \to 0} \Big[i \frac{e^2}{\Omega\beta} \frac{\hbar}{\mathcal{A}} \sum_{l \in \mathbb{Z}} \sum_{\mathbf{k}} \mathrm{Tr}[\hat{v}_x \hat{G}(\mathbf{k}, \Omega_l) \times \hat{v}_x \hat{G}(\mathbf{k}, \Omega_n + \Omega_l)]_{\Omega_n \to \Omega + i\delta} \Big] \tag{3.6}$$

Using the components of the velocity operator along the μ direction as $\hat{v}_\mu(\mathbf{k}) = \frac{1}{\hbar}\partial H/\partial k_\mu$, we get

$$\begin{aligned} \hat{v}_x(\mathbf{k}) &= 2t_0\sigma_0 k_x + 2t_j k_y \sigma_z + \lambda_1 \sigma_y \\ \hat{v}_y(\mathbf{k}) &= 2t_0\sigma_0 k_y + 2t_j k_x \sigma_z - \lambda \sigma_x \end{aligned} \tag{3.7}$$

From Eqn(3.1) we can find Matsubara Green's function using the relation $G = [i\Omega_n\sigma_0 - H]^{-1}$.which in the matrix form is obtained as-

$$\begin{pmatrix} \frac{k^2t-i\Omega_n-2k^2tj\cos(\theta)\sin(\theta)}{\frac{k^4}{2}(-2t^2+t_j^2)+\Omega_n^2+k^2(\lambda^2+2it\Omega_n)-\frac{1}{2}k^4t_j^2\cos(4\theta)} & \frac{k\lambda(i\cos(\theta)+\sin(\theta))}{\frac{k^4}{2}(-2t^2+t_j^2)+\Omega_n^2+k^2(\lambda^2+2it\Omega_n)-\frac{1}{2}k^4t_j^2\cos(4\theta)} \\ \frac{k\lambda(-i\cos(\theta)+\sin(\theta))}{\frac{k^4}{2}(-2t^2+t_j^2)+\Omega_n^2+k^2(\lambda^2+2it\Omega_n)-\frac{1}{2}k^4t_j^2\cos(4\theta)} & \frac{k^2t-i\Omega_n+2k^2tj\cos(\theta)\sin(\theta)}{\frac{k^4}{2}(-2t^2+t_j^2)+\Omega_n^2+k^2(\lambda^2+2it\Omega_n)-\frac{1}{2}k^4t_j^2\cos(4\theta)} \end{pmatrix}$$

or we can also write Green function in terms of pauli matrices.

$$G = \sum_s \left(\sigma_0 + s\frac{k^2t_j\sin 2\theta}{\Delta k}\sigma_z + s\lambda\frac{k_x\sigma_y - k_y\sigma_x}{\Delta k}\right)\cdot\frac{1}{2}\frac{1}{i\Omega - E_s + i\frac{\Gamma}{2}Sgn[\Omega_n]} \quad (3.8)$$

where the term $\frac{1}{2}\frac{1}{i\Omega - E_s + i\frac{\Gamma}{2}Sgn[\Omega_n]}$ will be taken as G_{0s}. Now from Eqn (3.6, 3.7 and 3.8) we can write

$$\begin{aligned} &Tr[v_\alpha(k)G(k,\Omega_l)v_\beta(k)G(k,\Omega_n+\Omega_l)] = \\ &\frac{1}{4}\sum_{s,s'}\left[v_\alpha\cdot\left(\sigma_0 + s\frac{k^2t_j\sin 2\theta}{\sqrt{\lambda^2k^2 - k^2t_j\sin^2 2\theta}}\sigma_z + s\lambda\frac{k_x\sigma_y - k_y\sigma_x}{\sqrt{\lambda^2k^2 - k^2t_j\sin^2 2\theta}}\right)\right] \\ &v_\beta\left(\sigma_0 + s'\frac{k^2t_j\sin 2\theta}{\sqrt{\lambda^2k^2 - k^2t_j\sin^2 2\theta}}\sigma_z + s'\lambda\frac{k_x\sigma_y - k_y\sigma_x}{\sqrt{\lambda^2k^2 - k^2t_j\sin^2 2\theta}}\right)]\cdot \\ &G_{0s}(k,\Omega_l)G_{0s'}(k,\Omega_l+\Omega_n) \end{aligned} \quad (3.9)$$

which gives us

$$\begin{aligned} &\sum_{l\in\mathbb{Z}}\mathrm{Tr}[\hat{v}_\mu(\mathbf{k})\hat{G}(\mathbf{k},\Omega_l)\hat{v}_\mu(\mathbf{k})\hat{G}(\mathbf{k},\Omega_l+\Omega_n)] \\ &= \mathcal{F}_\chi(\mathbf{k})\sum_{s,s'}\sum_{l\in\mathbb{Z}}G_0^s(\mathbf{k},\Omega_l)G_0^{s'}(\mathbf{k},\Omega_l+\Omega_n) \end{aligned} \quad (3.10)$$

as evident from Eqn(2.22) from previous discussion.To find the form of $\mathcal{F}_\chi(\mathbf{k})$ for our system we solve Eqn.(3.9) and obtain.

$$\begin{aligned} &Tr[v_\mu G(k,\Omega_l)\,v_\mu G(k,\Omega_n+\Omega_l)] = \\ &\frac{\lambda^2\left(3k^4tj^2 + k^2\lambda^2 \mp k^2\left(4k^2t_j^2+\lambda^2\right)\cos 2\theta + k^4tj^2\,\mathrm{Cos}[4\theta]\right)}{2\hbar^2\left(k^2\lambda^2 + k^2tj\sin 2\theta\left(k^2tj\sin 2\theta\right)\right)} \\ &\times G_{0s}(k,\Omega_l)\,G_{0s'}(k,\Omega_l+\Omega_n) \end{aligned} \quad (3.11)$$

comparing from Eqn[3.10] we get

$$\begin{aligned}\mathcal{F}_\chi \quad & (\mathbf{k}) = \mathrm{Tr}[\hat{v}_x(\sigma_0 + \boldsymbol{\sigma}\mathbf{g})\hat{v}_x(\sigma_0 - \boldsymbol{\sigma}\mathbf{g})] \\ = \quad & \frac{\lambda^2[t_j^2 k^4(2+\cos^2 2\phi_{\mathbf{k}}) + \lambda^2 k^2 - \chi k^2(\lambda^2 + 4t_j^2 k^2)\cos 2\phi_{\mathbf{k}}]}{2\hbar(\lambda^2 k^2 + t_j^2 k^4 \sin^2 2\phi_{\mathbf{k}})}. \end{aligned} \tag{3.12}$$

Here $\chi = +$ and $-$ for the component of the tensor when $\mu = x$ and $\mu = y$, respectively. Now, from Eqn[3.6] and Eqn[3.11] it is clear that we have to calculate $\left[\frac{1}{\beta}\sum_l G_0^s(\mathbf{k},\Omega_l)G_0^{s'}(\mathbf{k},\Omega_l+\Omega_n)\right]_{i\Omega_l\to\Omega+i\delta}$ which we denote by $I^n_{s,s'}(k)$.

Analytical continuation: To evaluate the summation over ($l \in \mathbb{Z}$) we take

$$\begin{aligned} I^n_{s,s'}(\mathbf{k}) &= \frac{1}{\beta}\sum_{l\in\mathbb{Z}} G_0^s(\mathbf{k},\Omega_l)G_0^{s'}(\mathbf{k},\Omega_l+\Omega_n) \\ &= \frac{1}{\beta}\sum_{l\in\mathbb{Z}} \frac{1}{i\Omega_l - E_s(\mathbf{k}) + i\frac{\Gamma}{2}\mathrm{sgn}(\Omega_l)} \\ &\times \frac{1}{i(\Omega_l+\Omega_n) - E_{s'}(\mathbf{k}) + i\frac{\Gamma}{2}\mathrm{sgn}(\Omega_l+\Omega_n)}. \end{aligned} \tag{3.13}$$

Using the standard Analytical continuation,

$$\frac{1}{\beta}\sum_{l=-\infty}^{\infty} g\left(i\Omega_l\right) = \frac{1}{2\pi i}\int_C dz\, \frac{g(z)}{^{\beta z}+1} \tag{3.14}$$

Recall,$E_k^s = k^2 t + s\sqrt{k^2 tj^2 \sin[2\theta]^2 + \lambda^2}$. from above two eqn we get

$$\begin{aligned} I^n_{s,s'}(\mathbf{k}) = -\frac{1}{2\pi i}\int_C dz f(z) & \frac{1}{i\Omega_l - E_s(\mathbf{k}) + i\frac{\Gamma}{2}\mathrm{sgn}(\Omega_l)} \\ \times & \frac{1}{i(\Omega_l+\Omega_n) - E_{s'}(\mathbf{k}) + i\frac{\Gamma}{2}\mathrm{sgn}(\Omega_l+\Omega_n)} \end{aligned}$$

where $i\Omega_l =$ z , $f(z)$ is the Fermi Dirac distribution function.

Now Defining

$$F(z) = \frac{1}{2\pi i} f(z) \frac{1}{[z - E_k^s + i\frac{\Gamma}{2}sgn(Im(z))][z + i\Omega_n - E_k^{s'} + i\frac{\Gamma}{2}Sgn(Im(z)) + \Omega_n]}$$

we can write-

$$I^n_{s,s'}(\mathbf{k}) = \frac{1}{2\pi i}\int_C dz f(z)\frac{1}{[z - E^s_k + i\frac{\Gamma}{2}sgn(Im(z))]}$$
$$\frac{1}{[z + i\Omega_n - E^{s'}_k + i\frac{\Gamma}{2}sgn(Im(z)) + \Omega_n]} = Res[f(z)]_{z=i\Omega_l} \qquad (3.15)$$

To Find the residue in above equation we have to identify the branch points:

1- One is the real axis due to $\frac{1}{z-E_k}$

2- The other is a line parallel to real axis at Im $[z] = -i\Omega_n$.

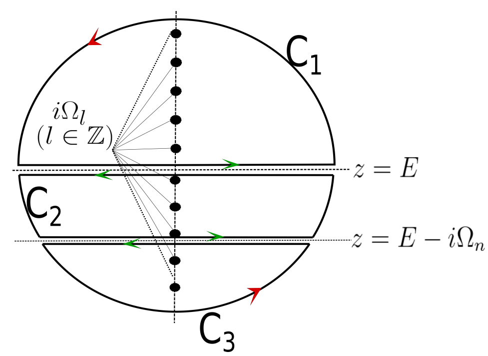

Figure 3.2: The different contours for the complex Matsubara frequency summation: The horizontal lines Im$(z) = 0$ and Im$(z) = -i\Omega_n$ denote the two branch cuts in the complex plane. The three contours of integration C_1, C_2, and C_3. The dots about the imaginary axis gives the poles of the Fermi-Dirac distribution function $f(z)$ which helps in deriving the analytical continuation in Eq. [3.16].

Poles of f(z) about the imaginary axis is given by the roots of the equation $e^{\beta z+1=0}$. since $e^{i\pi(2l+1)} = -1$ for all 'l',$e^{\beta z} = e^{\beta i\frac{\pi(2l+1)}{\beta}}$.

$$Res[F(z)]_{z=i\Omega_l}$$
$$= \lim_{z\to i\Omega_l+\eta}\frac{(z - i\Omega_l)}{(e^{\beta z+1})[z - E^s_k + i\frac{\Gamma}{2}Sgn(Im(z))][z + i\Omega_n - E^{s'}_k + i\frac{\Gamma}{2}Sgn(Im(z)) + \Omega_n]}$$
$$= \lim_{\eta\to 0}\left[\frac{1}{(e^{\beta i\Omega_l}e^{\beta\eta} + 1)[i\Omega_l + \eta - E^s_k + i\frac{\Gamma}{2}Sgn(Im(z))]}\right.$$
$$\left.\times\frac{(i\Omega_l + \eta - i\Omega_l)}{[i\Omega_l + \eta + i\Omega_n - E^{s'}_k + i\frac{\Gamma}{2}Sgn(Im(z)) + \Omega_n]}\right]$$

Using the limit $\eta = 0$ we get $\frac{\eta}{-e^{(\beta\eta+1)}+1} = -\frac{1}{\beta}$ thus we can finally write -

$$
\begin{aligned}
&Res[F(z)]_{z=i\Omega_l} = \frac{-1}{\beta}\frac{1}{[i\Omega_l - E_k^s + i\frac{\Gamma}{2}Sgn(Im(z))]} \\
&\times\frac{1}{[i\Omega_l + i\Omega_n - E_k^{s'} + i\frac{\Gamma}{2}Sgn(Im(z)) + \Omega_n]} \\
&= -I^n_{s,s'}(\mathbf{k})
\end{aligned}
$$

now i can write

$$
\begin{aligned}
&I^n_{s,s'}(\mathbf{k}) = \frac{-1}{2\pi i}\int_c f(z)\frac{1}{[i\Omega_l - E_k^s + i\frac{\Gamma}{2}Sgn(Im(z))]} \\
&\times\frac{1}{[i\Omega_l + i\Omega_n - E_k^{s'} + i\frac{\Gamma}{2}Sgn(Im(z)) + \Omega_n]}
\end{aligned}
$$

Thus, using the standard analytical continuation-

$$
\frac{1}{\beta}\sum_{l=-\infty}^{\infty} g(i\Omega_l) = \frac{1}{2\pi i}\oint_C dz f(z) g(z)
$$

with $f(z) = 1/(e^{\beta z}+1)$,we have-

$$
\begin{aligned}
I^n_{s,s'}(\mathbf{k}) &= \frac{1}{2\pi i}\oint_C \frac{f(z)}{z - E_s(\mathbf{k}) + i\frac{\Gamma}{2}\mathrm{sgn}[\mathrm{Im}(z)]} \\
&\times\frac{1}{z + i\Omega_n - E_{s'}(\mathbf{k}) + i\frac{\Gamma}{2}\mathrm{sgn}[\mathrm{Im}(z) + \Omega_n]}.
\end{aligned} \tag{3.16}
$$

Consider the integral to be integrated over the closed contour as shown in Fig. [3.2]. In order to evaluate the integral on the right hand side of the above Eq.[3.16], we modify the contour to be a sum of the closed paths C_1, C_2, and C_3 in order to avoid the two mentioned branch cuts (refer to Fig. [3.2]). By extending the contour to infinity, the integral in Eqn. [3.16] can be evaluated about the horizontal paths (shown by the green arrows). Thus we can change the integration variable in the above equation to $z = E + i\eta$ for the horizontal line in C_1, ($z = E - i\eta$ and $z = E - i\Omega_n + i\eta$ about the two horizontal lines in C_2) and $z = E - i\Omega_n - i\eta$ for the horizontal line in C_3, where $\eta \to 0$ is a positive infinitesimal number.

$$\frac{-1}{2\pi i}\int_c f(z)\frac{1}{[i\Omega_l - E_k^s + i\frac{\Gamma}{2}\mathrm{sgn}(Im(z))][i\Omega_l + i\Omega_n - E_k^{s'} + i\frac{\Gamma}{2}\mathrm{sgn}(Im(z)) + \Omega_n]}$$

$$= \frac{1}{2\pi i}\left[\int_{-\infty}^{\infty} dE\, f(E)\frac{1}{(E + i\eta - E_k^s + i\frac{\Gamma}{2})(E + i\Omega_n - E_k^{s'} + i\frac{\Gamma}{2}\mathrm{sgn}(\Omega_n))}\right.$$
$$+ \int_{-\infty}^{\infty} dE\, f(E)\frac{1}{(E - i\eta - E_k^s - i\frac{\Gamma}{2})(E + i\Omega_n - E_k^{s'} + i\frac{\Gamma}{2}\mathrm{sgn}(\Omega_n))}$$
$$+ \int_{-\infty}^{\infty} dE\, f(E)\frac{1}{(E + i\eta - E_k^s + i\frac{\Gamma}{2})(E - i\Omega_n - E_k^{s'} + i\frac{\Gamma}{2}\mathrm{sgn}(-i\Omega_n))}$$
$$\left.+ \int_{-\infty}^{\infty} dE\, f(E)\frac{1}{(E - i\eta - E_k^s - i\frac{\Gamma}{2})(E - i\Omega_n - E_k^{s'} + i\frac{\Gamma}{2}\mathrm{sgn}(-i\Omega_n))}\right]$$

further simplifying, we obtain

$$= \frac{1}{2\pi i}\int_{-\infty}^{\infty} dE\, f(E)\left(\frac{1}{(E - i\eta - E_k^s - i\frac{\Gamma}{2})(E + i\Omega_n - E_k^{s'} + i\frac{\Gamma}{2}\mathrm{sgn}(\Omega_n))}\right.$$
$$\left.+ \frac{1}{(E + i\eta - E_k^s + i\frac{\Gamma}{2})(E + i\Omega_n - E_k^{s'} + i\frac{\Gamma}{2}\mathrm{sgn}(\Omega_n))}\right)$$
$$+ \frac{1}{2\pi i}\int_{-\infty}^{\infty} dE\, f(E - i\Omega_n)\left(\frac{1}{(E + i\eta - E_k^{s'} + i\frac{\Gamma}{2})(E - i\Omega_n - E_k^s + i\frac{\Gamma}{2}\mathrm{sgn}(-\Omega_n))}\right.$$
$$\left.+ \frac{1}{(E - i\eta - E_k^{s'} - i\frac{\Gamma}{2})(E - i\Omega_n - E_k^s + i\frac{\Gamma}{2}\mathrm{sgn}(-\Omega_n))}\right) \quad (3.17)$$

further simplifying we get

$$= \frac{1}{2\pi i}\left[\int_{-\infty}^{\infty} dE\, f(E)\left(\frac{1}{(E + i\eta - E_k^s + i\frac{\Gamma}{2})} + \frac{1}{(E - i\eta - E_k^s - i\frac{\Gamma}{2})}\right)\right.$$
$$\times \frac{1}{E + i\Omega_n - E_k^{s'} + i\frac{\Gamma}{2}\mathrm{sgn}(\Omega_n)}$$
$$+ \int_{-\infty}^{\infty} dE\, f(E - i\Omega_n)\left(\frac{1}{(E + i\eta - E_k^{s'} + i\frac{\Gamma}{2})} + \frac{1}{(E - i\eta - E_k^{s'} - i\frac{\Gamma}{2})}\right)$$
$$\left.\times \frac{1}{E + i\Omega_n - E_k^s + i\frac{\Gamma}{2}\mathrm{sgn}(\Omega_n)}\right] \quad (3.18)$$

$$= -\frac{1}{2\pi}\int_{-\infty}^{\infty} dE \Bigg[\frac{\Gamma}{(E-E_k^s)^2+(\frac{\Gamma}{2})^2}\frac{f(E)}{E+i\Omega_n-E_k^{s'}+i\frac{\Gamma}{2}sgn[\Omega_n]}$$

$$+\frac{\Gamma}{(E-E_k^{s'})^2+(\frac{\Gamma}{2})^2}\frac{f(E-i\Omega_n)}{E-i\Omega_n-E_k^{s'}+i\frac{\Gamma}{2}sgn[\Omega_n]}\Bigg] \tag{3.19}$$

Thus the integral in Eq. [3.16] is

$$\oint_C \frac{f(z)dz}{(z-E_s(\mathbf{k})+i\frac{\Gamma}{2}\mathrm{sgn}[\mathrm{Im}(z)])(z+i\Omega_n-E_{s'}(\mathbf{k})+i\frac{\Gamma}{2}\mathrm{sgn}[\mathrm{Im}(z)+\Omega_n])}$$
$$= -\int_{-\infty}^{\infty} dE f(E)\Big[\frac{i\Gamma}{(E-E_s([\mathbf{k}))^2+(\Gamma/2)^2][E+i\Omega_n-E_{s'}(\mathbf{k})+i\Gamma/2]}$$
$$+\frac{i\Gamma}{[(E-E_{s'}(\mathbf{k}))^2+(\Gamma/2)^2][E-i\Omega_n-E_s(\mathbf{k})-i\Gamma/2]}\Big]. \tag{3.20}$$

We next change the integration variable $E \to E - E_s(\mathbf{k})$ in the first term and $E \to -E + E_{s'}(\mathbf{k})$ in the second term and obtained

$$I^n_{s,s'}(\mathbf{k}) = -\frac{1}{2\pi}\lim_{\eta\to 0}\int_{-\infty}^{\infty} dE \frac{\Gamma}{E^2+(\Gamma/2)^2}$$
$$\times\Big[\frac{f(E+E_s(\mathbf{k}))-f(-E+E_{s'}(\mathbf{k}))}{E+i\Omega_n+E_s(\mathbf{k})-E_{s'}(\mathbf{k})+i\Gamma/2}\Big]_{i\Omega_n\to\Omega+i\eta} \tag{3.21}$$

Case I ($s \neq s'$): (*Inter-band optical transition*) In this case the level broadening $\Gamma << \Omega$, such that

$$\begin{aligned} I^n_{s,s'}(\mathbf{k}) &= -\int_{-\infty}^{\infty} dE\delta(E)\frac{f(E+E_s(\mathbf{k}))-f(-E+E_{s'}(\mathbf{k}))}{E+\Omega+E_s(\mathbf{k})-E_{s'}(\mathbf{k})+i\Gamma/2} \\ &= -\frac{f(E_s(\mathbf{k}))-f(E_{s'}(\mathbf{k}))}{\Omega+E_s(\mathbf{k})-E_{s'}(\mathbf{k})+i\Gamma/2}. \end{aligned} \tag{3.22}$$

Also, we have

$$\begin{aligned} \mathrm{Im}[I^n_{s,s'}(\mathbf{k})]_{\imath\Omega_n\to\Omega+i\eta} &= \pi\Big[f(E_s(\mathbf{k}))-f(E_{s'}(\mathbf{k}))\Big] \\ &\times \delta(\Omega+E_s(\mathbf{k})-E_{s'}(\mathbf{k})), \end{aligned} \tag{3.23}$$

where we define $\delta(x) = \frac{1}{\pi}\frac{\Gamma/2}{x^2+(\Gamma/2)^2}$. Recall Eqn[3.11],then using Eqn(3.21) we can write-

$$\begin{aligned}
&\sigma_{\frac{x}{y},\frac{x}{y}} = i\frac{e^2}{\Omega}\frac{1}{(2\pi)^2} \\
&\times \lim_{\delta\to 0}\sum_{s,sp}\int_{BZ} d^2k \frac{\lambda^2\left(3k^4tj^2 + k^2\lambda^2 \mp k^2\left(4k^2tj^2+\lambda^2\right)\cos(2\theta) + k^4tj^2\cos(4\theta)\right)}{2\hbar^2\left(k^2\lambda^2 + k^2tj\sin(2\theta)\left(k^2tj\sin(2\theta)\right)\right)} \\
&\times \frac{[f(E_k^s) - f(E_k^{s'})]}{E_k^s + \Omega - E_k^{s'} + i\frac{\Gamma}{2}}
\end{aligned} \tag{3.24}$$

using Eqn[3.23] we obtain the real part of equation -

$$\begin{aligned}
&\mathrm{Re}[\sigma_{\frac{x}{y},\frac{x}{y}}] = i\frac{e^2}{\Omega}\frac{1}{(2\pi)^2} \\
&\times \sum_{ss'}\int dk \frac{\lambda^2\left(3k^4tj^2 + k^2\lambda^2 \mp k^2\left(4k^2tj^2+\lambda^2\right)\cos(2\theta) + k^4tj^2\cos(4\theta)\right)}{2\hbar^2\left(k^2\lambda^2 + k^2tj\sin(2\theta)\left(k^2tj\sin(2\theta)\right)\right)} \\
&\times [f(E_s^k) - f(E_k^{s'})]\cdot \pi\delta(\Omega - E_k^{s'} + E_s^k)
\end{aligned}$$

Now,

$$\delta(\Omega - E_k^{s'} + E_k^s) = \delta(\Omega - 2\sqrt{\lambda^2k^2 + (\Delta z - k^2t_j\sin 2\theta)^2}) = \frac{\delta(k-k_\Omega)}{\frac{2k(\lambda^2+2t_j\sin 2\theta(-\Delta z+k^2t_j\sin 2\theta))}{\sqrt{k^2\lambda^2+(\Delta z-k^2t_j\sin 2\theta)^2}}}$$

where k_Ω is the root of the equation $\Omega - 2\sqrt{\lambda^2k^2 + (\Delta z - k^2t_j\sin 2\theta)^2} = 0$. Simplifying the above equation and putting the values given above we obtain

$$\begin{aligned}
Re[\sigma_{\frac{x}{y},\frac{x}{y}}] = i\frac{e^2}{\Omega}\frac{1}{(2\pi)^2}\sum_{s,s'}\int dk \frac{\lambda^2(2k^2t_j^2 + \lambda^2 - 2k^2t_j^2\cos 2\theta\sin^2\theta)}{\hbar^2(\lambda^2 + k^2t_j^2\sin^2 2\theta)} \\
\times [f(E_s^k) - f(E_k^{s'})]\frac{\delta(k-k_\Omega)}{\frac{2k(\lambda^2+2t_j\sin 2\theta(-\Delta z+k^2t_j\sin 2\theta))}{\sqrt{k^2\lambda^2+(\Delta z-k^2t_j\sin 2\theta)^2}}}
\end{aligned} \tag{3.25}$$

Now, the integral in Eq.[3.25], can thus be written as

$$\begin{aligned}
\mathrm{Re}[\sigma_{xx}(\Omega)] &= \frac{e^2}{4\pi}\frac{\hbar}{\Omega}\sum_{s\neq s'}\int \mathbf{dk}\mathcal{F}_+(\mathbf{k})\Big[f(E_s(\mathbf{k})) - f(E_{s'}(\mathbf{k}))\Big] \\
&\times \delta(\Omega + E_s(\mathbf{k}) - E_{s'}(\mathbf{k})).
\end{aligned} \tag{3.26}$$

Case II ($s = s'$): (*Intra-band optical transition*) In this case, we have Eqn. [3.21] written as

$$\begin{aligned}
\mathrm{Im}[I^n_{s,s}(\mathbf{k})]_{\imath\Omega_n\to\Omega+i\eta} &= \frac{1}{2}\int_{-\infty}^{\infty} dE \frac{\Gamma}{E^2+(\Gamma/2)^2} \\
\times & \quad \delta(E+\Omega)[f(E+E_s(\mathbf{k}))-f(-E+E_s(\mathbf{k}))] \\
= & \quad \frac{\Gamma/2}{\Omega^2+(\Gamma/2)^2}[f(-\Omega+E_s(\mathbf{k}))-f(\Omega+E_s(\mathbf{k}))] \\
= & \quad \pi\delta(\Omega)[f(-\Omega+E_s(\mathbf{k}))-f(\Omega+E_s(\mathbf{k}))] \qquad (3.27)
\end{aligned}$$

In a similar way we get,

$$\begin{aligned}
\mathrm{Re} \quad [\sigma_{xx}(\Omega)] &= \frac{e^2}{4\pi}\frac{\hbar}{\Omega}\sum_s \int \mathbf{dk}\mathcal{G}(\mathbf{k})\delta(\Omega) \\
\times & \quad [f(-\Omega+E_s(\mathbf{k}))-f(\Omega+E_s(\mathbf{k}))], \qquad (3.28)
\end{aligned}$$

where

$$\mathcal{G}(\mathbf{k}) = \mathrm{Tr}[\hat{v}_x(\sigma_0+\boldsymbol{\sigma}\mathbf{g})\hat{v}_x(\sigma_0-\boldsymbol{\sigma}\mathbf{g})] \qquad (3.29)$$

Calculation of the Hall conductivity: The anisotropic even-parity characteristic of the Berry curvature also promt us to carry out the calculation of the non-diagonal (Hall) component of the conductivity tensor. We again use the Kubo formula within the linear response regime where the transversal conductivity in a quantum Hall channel can be written as.

$$\begin{aligned}
\sigma_{xy}(\Omega) &= \lim_{\delta\to 0}\Big[\frac{e^2}{\Omega\beta}\mathcal{A}\sum_{l\in\mathbb{Z}}\sum_{\mathbf{k}}\mathrm{Im}\{\mathrm{Tr}[\hat{v}_x\hat{G}(\mathbf{k},\Omega_l) \\
& \times \quad \hat{v}_y\hat{G}(\mathbf{k},\Omega_n+\Omega_l)]\}\Big]_{\Omega_n\to\Omega+i\delta} \qquad (3.30)
\end{aligned}$$

The quantity $\mathrm{Im}\{\mathrm{Tr}[\hat{v}_x\hat{G}(\mathbf{k},\Omega_l)\hat{v}_y\hat{G}(\mathbf{k},\Omega_n+\Omega_l)]\}$ can be worked out as-

$$\begin{aligned}
& \mathrm{Im}\{\mathrm{Tr}[\hat{v}_x\hat{G}(\mathbf{k},\Omega_l)\hat{v}_y\hat{G}(\mathbf{k},\Omega_n+\Omega_l)]\} = \\
& \sum_{s\neq s'} s\frac{\lambda^2(\Delta_z+t_jk^2\sin 2\phi_{\mathbf{k}})}{\hbar^2\Delta_{\mathbf{k}}}G_0^s(\mathbf{k},\Omega_n)G_0^{s'}(\mathbf{k},\Omega_n+\Omega_l)
\end{aligned}$$

Thus

$$\begin{aligned}
\sigma_{xy}(\Omega) &= \lim_{\delta\to 0}\Big[\frac{e^2}{\Omega\beta}\mathcal{A}\sum_{\mathbf{k}}\sum_{s\neq s'} s\frac{\lambda^2(\Delta_z+t_jk^2\sin 2\phi_{\mathbf{k}})}{\hbar^2\Delta_{\mathbf{k}}} \\
& \times \quad \sum_{l\in\mathbb{Z}} G_0^s(\mathbf{k},\Omega_n)G_0^{s'}(\mathbf{k},\Omega_n+\Omega_l)\Big]_{\Omega_n\to\Omega+i\delta}, \qquad (3.31)
\end{aligned}$$

From Eq. [3.16 & 3.20] , $\sum_{l\in\mathbb{Z}} G_0^s(\mathbf{k},\Omega_n)G_0^{s'}(\mathbf{k},\Omega_n+\Omega_l) = \beta\frac{f_{s'}-f_s}{E_s-E_{s'}+i\Omega_n}$

$$\begin{aligned}\sigma_{xy}(\Omega) &= -\lim_{\delta\to 0}\Big[\frac{e^2}{\Omega}\mathcal{A}\sum_{\mathbf{k}}\sum_{s\neq s'} s\frac{\lambda^2(\Delta_z+t_jk^2\sin 2\phi_{\mathbf{k}})}{\hbar^2\Delta_{\mathbf{k}}} \\ &\times \frac{f_s-f_{s'}}{E_s-E_{s'}+i\Omega_n}\Big]_{\Omega_n\to\Omega+i\delta} \end{aligned} \tag{3.32}$$

The imaginary part of $\sigma_{xy}(\Omega)$ can be obtained as

$$\begin{aligned}\mathrm{Im}[\sigma_{xy}(\Omega)] &= \frac{e^2\lambda^2}{4\pi^2\Omega}\sum_{s\neq s'} s\int \mathbf{dk}\frac{\Delta_z+t_jk^2\sin[2(\eta+\phi_{\mathbf{k}})]}{\Delta_k^3} \\ &\times \delta(E_s(\mathbf{k})-E_{s'}(\mathbf{k})-\Omega). \end{aligned} \tag{3.33}$$

DC limit: Using the L'Hospital's rule,

$$\lim_{\Omega\to 0}\frac{[\sigma_{xy}(\Omega)]}{\Omega} = \Big[\frac{d\sigma_{xy}(\Omega)}{d\Omega}\Big]_{\Omega\to 0} \tag{3.34}$$

the DC limit can be obtained from Eqn. [3.32]

$$\begin{aligned}\sigma_{xy} &= -\lim_{\delta\to 0}\Big[e^2\mathcal{A}\sum_{\mathbf{k}}\sum_{s\neq s'} s\frac{\lambda^2(\Delta_z+t_jk^2\sin 2\phi_{\mathbf{k}})}{\hbar^2\Delta_{\mathbf{k}}} \\ &\times (f_s-f_{s'})\lim_{\Omega\to 0}\frac{d}{d\Omega}\Big[\frac{1}{\Omega+i\delta+E_s-E_{s'}}\Big]\Big] \end{aligned} \tag{3.35}$$

also

$$\lim_{\delta\to 0}[\lim_{\Omega\to 0}\frac{d}{d\Omega}\Big[\frac{1}{\Omega+i\delta+E_s-E_{s'}}\Big]] = -\frac{1}{(E_s-E_{s'})^2} \tag{3.36}$$

Thus

$$\sigma_{xy} = e^2\mathcal{A}\sum_{\mathbf{k}}\sum_{s\neq s'}(f_s-f_{s'})s\frac{\lambda^2(\Delta_z+t_jk^2\sin 2\phi_{\mathbf{k}})}{4\hbar^2\Delta_{\mathbf{k}}^3}$$

If the Fermi level is lying in between E_s and $E_{s'}$,

$$\sigma_{xy} = e^2\mathcal{A}\sum_{\mathbf{k}}\sum_{s\neq s'} s\frac{\lambda^2(\Delta_z+t_jk^2\sin 2\phi_{\mathbf{k}})}{4\hbar^2\Delta_{\mathbf{k}}^3} \tag{3.37}$$

The term inside the summation on the RHS is the Berry curvature.

$$\begin{aligned}\sigma_{xy}(\Omega) &= \lim_{\delta\to 0}\Big[\frac{e^2}{\Omega\beta}\mathcal{A}\sum_{l\in\mathbb{Z}}\sum_{\mathbf{k}}\mathrm{Im}\{\mathrm{Tr}[\hat{v}_x\hat{G}(\mathbf{k},\Omega_l) \\ &\times \hat{v}_y\hat{G}(\mathbf{k},\Omega_n+\Omega_l)]\}\Big]_{\Omega_n\to\Omega+i\delta}, \end{aligned} \tag{3.38}$$

thus the above calculations give us -

$$\begin{aligned}\mathrm{Im}[\sigma_{xy}](\Omega) &= \frac{e^2}{h}\frac{\lambda^2}{2\Omega}\sum_{s\neq s'} s\int \mathbf{dk}\frac{\Delta_z + t_j k^2\sin 2\phi_{\mathbf{k}}}{\Delta_{\mathbf{k}}^2} \\ &\times \quad \delta(\Omega - E_s(\mathbf{k}) + E_{s'}(\mathbf{k})). \end{aligned} \tag{3.39}$$

In the DC limit it can be shown that

$$\sigma_{xy} = \frac{e^2}{(2\pi)^2}\sum_{s\neq s'} s\int \mathbf{dk}\frac{\lambda^2(\Delta_z + t_j k^2\sin 2\phi_{\mathbf{k}})}{4\hbar^2\Delta_{\mathbf{k}}^3}. \tag{3.40}$$

For our analysis of the derived transport parameters, we set the parameters according to the table[3.1].

3.3 Result and discussion

From above derivation one of the diagonal elements of optical conductivity is given by

$$\begin{aligned}\mathrm{Re}[\sigma_{xx}(\Omega)] = \frac{e^2}{h}\Big[\frac{\lambda^2}{2\Omega^2}\sum_{s\neq s'}\int_{S_\Omega} dS_\Omega[f(E_s(\mathbf{k})) - f(E_{s'}(\mathbf{k})] \\ \times k_\Omega\frac{\lambda^2 + 4t_j^2k_\Omega^2\sin^2\phi_{\mathbf{k}}}{\lambda^2 + 2t_j^2k_\Omega^2\sin^2 2\phi_{\mathbf{k}}}\sin^2\phi_{\mathbf{k}}, + \frac{\hbar^2}{2\Omega}\delta(\Omega)\sum_{s=s'}\int \mathbf{dk}\ \mathcal{G}(\mathbf{k}) \\ \times[f(-\Omega + E_s(\mathbf{k})) - f(\Omega + E_s(\mathbf{k}))]\Big], \end{aligned} \tag{3.41}$$

where the integral in the first term is to be evaluated over the constant energy contour S_Ω, (shown in Fig. [3.1 (a)]) and where $k_\Omega(\phi_{\mathbf{k}})$ is the root of the Eq. $\Omega - E_+(k_\Omega, \phi_{\mathbf{k}}) + E_-(k_\Omega, \phi_{\mathbf{k}}) = 0$. The form of $\mathcal{G}(\mathbf{k})$ in the second term is given in Eqn. [3.29]. We also note that the first term is the contributions from the inter-band optical transitions and the intra-band contributions come from the second term which dominates in the low-frequency spectrum.

It must be mentioned that there's no anisotropy of the optical conductivity tensors, despite the anisotropy of the band induced by the parameter t_j. The inter-band optical transitions between the two level bands takes place when the photon energy, Ω is such that $E_g^+(\phi_{\mathbf{k}}) \leq \Omega \leq E_g^-(\phi_{\mathbf{k}})$, with $E_g^\pm(\phi_{\mathbf{k}})$ defined as $E_g^\pm = 2\sqrt{\lambda^2 {k_F^\pm}^2 + t_j^2 {k_F^\pm}^4\sin^2 2\phi_{\mathbf{k}}}$. Also, $k_F^\pm(\phi_{\mathbf{k}})$ are the Fermi wave-vectors

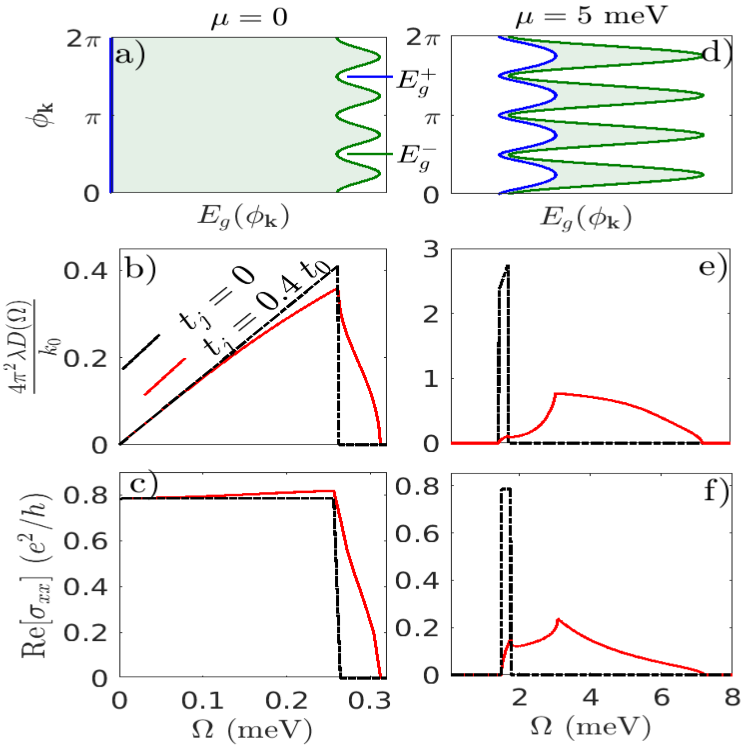

Figure 3.3: a) & d) Plots of the quantity $E_g(k_F^{\pm}(\phi_{\mathbf{k}}))$. The region between the red and blue curves gives the number of allowed states for optical transition. b) & e) are the joint density of states scaled to a dimensionless quantity $4\pi^2\lambda D(\Omega)/k_0$, taking $k_0 = 10^8$ m^{-1}. c) & f) the quantity $\sigma_{xx}(\Omega)$ (in units of e^2/h) for $\mu = 5$ meV in a) to c) and $\mu = 0$ in d) to f), respectively. An important observation, t_j increase the optical absorption spectra.

corresponding to the two spin-split states. In Fig. [3.3], we show the angular dependent of the quantities $E_g^{\pm}(\phi_{\mathbf{k}})$ in order to get a flavour of the available states (the shaded area between E_g^+ and E_g^-) given a spectrum of frequency, Ω. The role of the parameter t_j can also be seen as an enhancement of the optical spectrum which is evident from Fig. [3.3]. In Fig. [3.3], we have analyse the optical conductivity tuning the Fermi level to 0 [(a),(b),(c)] and 5 meV [(d),(e),(f)]. Also, the solid red curves are the characteristics of the optical conductivity when the alterferromagnetic parameter is introduced in the system, which increases the band width of the optical spectrum. This has an analoque of the Dresselhaus spin-orbit coupling discussed in Ref.[20] where a similar enhancement of the inter-band optical band-width is observed when it is introduced.

Before we dig deep into the behaviour of the optical conductivity tensor, let us calculate the joint density of states given by

$$\begin{aligned} D(\Omega) &= \frac{1}{\mathcal{A}}\sum_{s\neq s'\mathbf{k}}[f(E_s)-f(E_{s'})]\mathrm{Im}\Big[\frac{1}{\Omega-E_s+E_{s'}+i\delta}\Big] \\ &= \frac{1}{4\pi}\int_{S_\Omega} dS_\Omega \frac{f(E_s)-f(E_{s'})}{|\partial_k(E_s-E_{s'})|}\Big|_{k_\Omega}. \end{aligned} \tag{3.42}$$

We analyse this quantity numerically over a given spectrum of the frequency, taking the rest of parameters from table-I. The plot of the joint density of states is shown in Fig. [3.3 b) and f)]. From the above Eq., the joint density of states diverges when $|\partial_k(E_s-E_{s'})|_{k_\Omega}=0$ (often called as van Hove singular points) and that leads to a maximum probability for the optical transition. As seen in Fig. [3.3 (d & e)], the van Hove singular points occurs at several points in the Brillouin zone, *viz*, $(k_\Omega,(2n+1)\pi/4)$ and $(k_\Omega,n\pi/2)$. Clearly the points $(k_\Omega,(2n+1)\pi/4)$ are that corresponding to $E_g^+((2n+1)\pi/4)$, whereas $(k_\Omega,n\pi/2)$ that of $E_g^-(n\pi/2)$. Eivident from the plot that the optical conductivity follows the trails of the joint density of states.

3.4 Conclusion

We have shown that the spin-dependent coupling parameterized by t_j, i.e special to altermagnets, induces the huge band anisotropy in the system leading to the band width increment of the optical absorption spectrum. The ground state Hamiltonian for such a system is obtained by introducing Rashba spin-orbit coupling that is necessary to realize the d-wave nature of altermagnets (a counterpart of d-wave superconductivity). As the Fermi-level is increased the probability of the number of allowed states for optical transition decreases but the trend remains the same. We can also see that both the joint density of states and optical conductivity calculations are in the agreement with the result predicting the presence of Van-Hove singular points in various location in the Brillouin zone.

Enhancement of the frequency range is essential to encompass certain effects for studying topological phase such as Kerr and Faraday non-linearity. Also, our work is essential for several practical applications specially in the field of nanophotonics and spintronics. The enhanced optical absorption can lead to more sensitive photodetectors , ultra-compact and high performance optical devices.

Bibliography

[1] Libor Šmejkal, Jairo Sinova, and Tomas Jungwirth. Emerging research landscape of altermagnetism. *Physical Review X*, 12(4):040501, 2022.

[2] Helena Reichlová, Rafael Lopes Seeger, Rafael González-Hernández, Ismaila Kounta, Richard Schlitz, Dominik Kriegner, Philipp Ritzinger, Michaela Lammel, Miina Leiviskä, Václav Petříček, et al. Macroscopic time reversal symmetry breaking arising from antiferromagnetic zeeman effect. 2023.

[3] Hai-Yang Ma, Mengli Hu, Nana Li, Jianpeng Liu, Wang Yao, Jin-Feng Jia, and Junwei Liu. Multifunctional antiferromagnetic materials with giant piezomagnetism and noncollinear spin current. *Nature communications*, 12(1):2846, 2021.

[4] Libor Šmejkal, Jairo Sinova, and Tomas Jungwirth. Beyond conventional ferromagnetism and antiferromagnetism: A phase with nonrelativistic spin and crystal rotation symmetry. *Physical Review X*, 12(3):031042, 2022.

[5] WF Brinkman and Roger James Elliott. Theory of spin-space groups. *Proceedings of the Royal Society of London. Series A. Mathematical and Physical Sciences*, 294(1438):343–358, 1966.

[6] Daniel B Litvin and W Opechowski. Spin groups. *Physica*, 76(3):538–554, 1974.

[7] Lev Davidovich Landau, John Stewart Bell, MJ Kearsley, LP Pitaevskii, EM Lifshitz, and JB Sykes. *Electrodynamics of continuous media*, volume 8. elsevier, 2013.

[8] Louis Néel. Magnetism and local molecular field. *Science*, 174(4013):985–992, 1971.

[9] Sebastian Loth, Susanne Baumann, Christopher P Lutz, DM Eigler, and Andreas J Heinrich. Bistability in atomic-scale antiferromagnets. *Science*, 335(6065):196–199, 2012.

[10] Sergei A Egorov and Robert A Evarestov. Colossal spin splitting in the monolayer of the collinear antiferromagnet mnf2. *The Journal of Physical Chemistry Letters*, 12(9):2363–2369, 2021.

[11] Sergei A Egorov, Daniel B Litvin, and Robert A Evarestov. Antiferromagnetism-induced spin splitting in systems described by magnetic layer groups. *The Journal of Physical Chemistry C*, 125(29):16147–16154, 2021.

[12] EN Adams and EI Blount. Energy bands in the presence of an external force field—ii: Anomalous velocities. *Journal of Physics and Chemistry of Solids*, 10(4):286–303, 1959.

[13] Ming-Che Chang and Qian Niu. Berry curvature, orbital moment, and effective quantum theory of electrons in electromagnetic fields. *Journal of Physics: Condensed Matter*, 20(19):193202, 2008.

[14] David J Thouless, Mahito Kohmoto, M Peter Nightingale, and Marcel den Nijs. Quantized hall conductance in a two-dimensional periodic potential. *Physical review letters*, 49(6):405, 1982.

[15] Libor Šmejkal, Allan H MacDonald, Jairo Sinova, Satoru Nakatsuji, and Tomas Jungwirth. Anomalous hall antiferromagnets. *Nature Reviews Materials*, 7(6):482–496, 2022.

[16] Zexin Feng, Xiaorong Zhou, Libor Šmejkal, Lei Wu, Zengwei Zhu, Huixin Guo, Rafael González-Hernández, Xiaoning Wang, Han Yan, Peixin Qin, et al. An anomalous hall effect in altermagnetic ruthenium dioxide. *Nature Electronics*, 5(11):735–743, 2022.

[17] Igor I Mazin, Klaus Koepernik, Michelle D Johannes, Rafael González-Hernández, and Libor Šmejkal. Prediction of unconventional magnetism in doped fesb2. *Proceedings of the National Academy of Sciences*, 118(42):e2108924118, 2021.

[18] Makoto Naka, Satoru Hayami, Hiroaki Kusunose, Yuki Yanagi, Yukitoshi Motome, and Hitoshi Seo. Anomalous hall effect in κ-type organic antiferromagnets. *Physical Review B*, 102(7):075112, 2020.

[19] Adeline Crépieux and Patrick Bruno. Theory of the anomalous hall effect from the kubo formula and the dirac equation. *Physical Review B*, 64(1):014416, 2001.

[20] Jesús A Maytorena, Catalina López-Bastidas, and Francisco Mireles. Spin and charge optical conductivities in spin-orbit coupled systems. *Physical Review B*, 74(23):235313, 2006.